# Structural Characterization of β-Agostic Bonds in Pd-Catalyzed Polymerization

Hongwei Xu,[+] Chunhua Tony Hu,[+] Xiaoping Wang,[‡] and Tianning Diao[+,*]

[+]Department of Chemistry, New York University, 100 Washington Square East, New York, New York 10003, United States

[‡]Chemical and Engineering Materials Division, Oak Ridge National Laboratory, Oak Ridge, TN 37831, United States

*Supporting Information Placeholder*

**ABSTRACT:** β-Agostic Pd complexes play a critical role in controlling catalytic reactions, such as olefin polymerization and Heck reactions. Pd β-agostic complexes, however, have eluded structural characterization, due to the fact that these highly unstable molecules are difficulties to isolate. Herein, we report the single-crystal X-ray and neutron diffraction characterization of β-agostic (α-diimine)Pd-ethyl intermediates in polymerization. Short $C_\alpha$–$C_\beta$ distances and acute Pd–$C_\alpha$–$C_\beta$ bond angles combined serve as unambiguous evidence for the β-agostic interaction. Characterization of the agostic structure and the kinetic barrier for β-H elimination offer important insight into the fundamental understanding of agostic bonds and the mechanism of polymerization.

Agostic interactions are three-center, two-electron bonds formed between the empty d-orbital of a transition metal and a C–H bond of their alkyl ligands.[1] Agostic complexes are commonly assumed to be intermediates in catalytic reactions going through C–H activation[2] and β-H elimination steps.[3] Consequently, characterization of agostic bonds has attracted extensive interest.[1,4] Crystallography, including X-ray[5] and neutron diffraction,[6] serves as the key characterization method for agostic complexes. Among group 10 transition metals, single-crystal structures of Ni[7] and Pt[8] β-agostic complexes have been reported by us and others. In contrast, β-agostic Pd complexes have not been isolated and crystallographically analyzed due to their instability.[9] The difficulty of isolating β-agostic Pd complexes can be attributed to fast β-H elimination at the Pd center.

Cationic (α-diimine)Pd complexes display intriguing reactivity and properties in olefin polymerization.[10,11] Compared with Ziegler-Natta catalysts, (α-diimine)Pd catalysts are tolerant of many functional groups, enabling copolymerization of polar monomers that are incompatible with early transition metals.[12] In addition, (α-diimine)Pd catalysts allow for the formation of highly branched polyolefins, whereas branching is difficult to achieve with Ziegler-Natta catalysts.[13]

Mechanistic studies by Brookhart and coworkers identified β-agostic Pd complexes to be critical intermediates in directing branching in the polymerization of olefins (Scheme 1).[14,15] The formation of branched polymers is initiated by β-H elimination of the β-agostic Pd intermediate (step i), followed by olefin insertion to form the regio-isomer **B** (step ii). Repeating this process leads to migration of the Pd catalyst along the polymer chain. Intermediate **A** or **B** can reversibly coordinate with the alkene monomer upon cleavage of the agostic bonds (step iii). Once insertion of the monomer occurs, the chain propagates with branches. As a result, the stability of the β-agostic Pd complex **A** towards olefin coordination and β-H elimination determines the molecular weight and morphology of the polymer. Although β-agostic (α-diimine)Pd complexes have been observed by $^1$H NMR spectroscopy,[14] no crystallographic characterization has been obtained.

**Scheme 1. Mechanism of (α-diimine)Pd-Catalyzed Polymerization of Olefins**

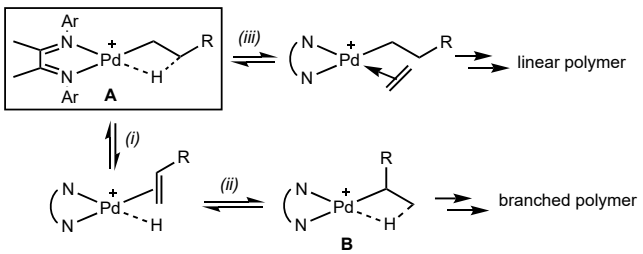


The long-standing interest in characterizing agostic interactions, in combination with the critical role of Pd β-agostic complexes in polymerization, prompted us to structurally characterize cationic (α-diimine)Pd agostic complexes. Herein, we report the single crystal X-ray and neutron diffraction structures of [(α-diimine)PdEt]$^+$ complexes, which reveal unambiguous proof of β-agostic bonds.

Our previous studies on (α-diimine)Ni agostic complexes revealed that a cyclohexyl backbone on the α-diimine ligand stabilized the molecule.[7c] We then applied this cyclohexyl backbone to Pd agostic complexes. Protonation of (α-diimine)$PdEt_2$ complex **1a** with

HBAr'$_4$ (Ar' = 3,5-$(CF_3)_2C_6H_3$)[16] afforded a dark red complex in 23% yield (Scheme 2). At –95 ºC, a solution of the new complex in $CD_2Cl_2$ exhibits two broad resonances in the $^1$H NMR spectrum at –8.8 ppm and 1.7 ppm in a 1:4 ratio. COSY experiment at –95 ºC indicated coupling between these two resonances (Figure S46). Comparing the NMR spectra with previous reports led us to assign the dark red complex to β-agostic Pd($CH_2CH_2$-$\mu$-H) cation **2a**.[14c] The use of **1a-*d*$_{10}$**, in which the ethyl groups are deuterated, formed the corresponding new complex **2a-*d*$_5$**. The $^1$H NMR spectrum of **2a-*d*$_5$** lacked resonances at –8.8 ppm and 1.7 ppm (Figure S1). The broad peak at –8.8 ppm is characteristic of an agostic proton,[1b,17] whereas the peak at 1.7 ppm is assigned to the coalescent signal of the β-non-agostic $^b$Hs and α-$^c$Hs. Simulation of the peak shape by gNMR revealed that the line broadening of the H resonances is a consequence of rapid exchange between $^b$H and $^c$H (Figure S2).[18]

**Scheme 2. Synthesis of β-H Agostic (α-diimine)Pd Complexes**

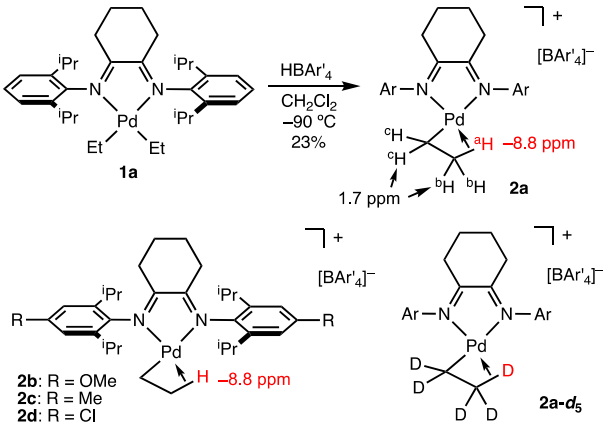


Substituents at the *para* position of the aromatic ring of the ligands have been reported to affect the molecular weight and branching morphology of polymer products.[19] Protonation of (α-diimine)$PdEt_2$ derivatives with different *para*-substituents by HBAr'$_4$ resulted in the formation of **2b**-**2d** (Scheme 1). While the electronic effect of the substituents led to noticeable shifts of the proton resonances of the Et group in complex **1**, it caused little change in the chemical shifts of the agostic protons of complex **2**. We attribute the similar chemical shifts of the agostic protons to the weaker agostic bonding interactions relative to a covalent bond.

Complex **2a** is an active intermediate for ethylene polymerization. The turnover number (TON) and turnover frequency (TOF) of **2a** in polymerization of ethylene are comparable to those of the original (α-diimine)Pd catalysts (Table 1).[10] The polyethylene generated by Pd catalysts has a dramatically higher degree of branching than that formed with analogous Ni catalysts.[7c] This different reactivity is attributed to faster β-H elimination and chain migration with Pd.[20]

**Table 1. Polymerization of Ethylene with 2a**

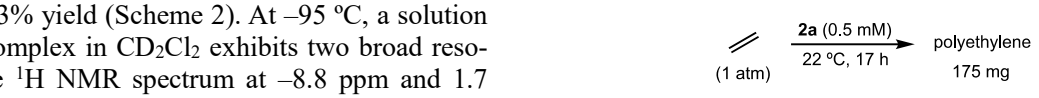


| TON | TOF ($h^{-1}$) | $M_n$[a] | $M_w$ | $M_w/M_n$ | branches per 1000 carbons |
|---|---|---|---|---|---|
| 5680 | 334 | 108000 | 225000 | 2.08 | 121 |

[a] Molecular weight data reported against polystyrene standards.

The stabilization provided by the cyclohexyl backbone allowed us to obtain single crystals of **2a**, **2b** and **2d** at –35 ºC that were suitable for single-crystal X-ray and neutron structure determination (Figure 1, *cf.* Figures S6-S7). In all structures, the trifluoromethyl groups of the BAr'$_4$ anions are disordered. The disorder led to difficulty in refining the structures to high agreement, but was inconsequential for assigning the well-ordered ethyl groups bound to Pd in **2a**·$CH_2Cl_2$ (Figure 1A). The position of the agostic hydrogen could not be located directly from the differential electron density map, due to the low electron intensity of the hydrogen atom in contrast to the heavy Pd atom. In order to precisely locate the agostic hydrogen, we conducted neutron diffraction analysis. A crystal of **2b**·$CH_2Cl_2$ (Figure 1B) suitable for neutron diffraction was chosen for measurement using the single crystal beamline TOPAZ of the Spallation Neutron Source. The position of the agostic hydrogen (H1Pd) in the major component of the crystal was located from the difference Fourier map, and its atomic displacement parameter was refined anisotropically (Figure 1C).

(A)

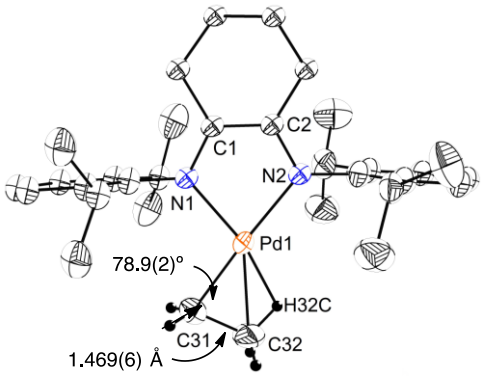


(B)

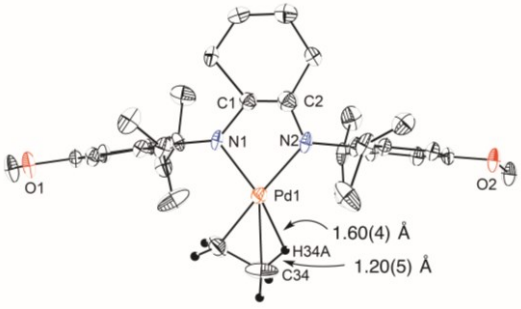

(C)

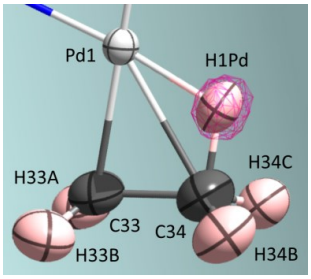


**Figure 1.** Molecular structures of agostic complexes. (A) X-ray structure of **2a**·$CH_2Cl_2$. Selected bond lengths (Å) and bond angles (º): C31–C32, 1.469(6); Pd–C31–C32, 78.9(2). (B) X-ray structure of **2b**·$CH_2Cl_2$. (C) Difference Fourier map showing the negative nuclear scattering density of the agostic hydrogen atom (H1Pd) of **2b**·$CH_2Cl_2$. Atom thermal ellipsoids are shown at the 50% probability level. The hydrogen atoms on the α-diimine ligands, $[BAr'_4]^-$, and $CH_2Cl_2$ are omitted for clarity.

The bond length of Pd–$C_\alpha$(C31) for **2a** is 2.030(4) Å, slightly longer than that of Ni–$C_\alpha$ in the analogous agostic complex (Table 2).[7c] The longer Pd–$C_\alpha$ bond length could be attributed to the larger nuclear radius of Pd relative to Ni. Correspondingly, the distance between Pd and $C_\beta$(C32) is longer than that of Ni. The bond length of $C_\alpha$–$C_\beta$ (C31–C32) for **2a** is 1.469(6) Å, which is shorter than that of the non-agostic Pd–Et complex, **1a** (1.528(3) Å, Figure S5), comparable to previous observations on analogous Ni agostic complexes.[7c] The decreased $C_\alpha$–$C_\beta$ bond length can be attributed to the greater $sp^2$ character of the $C_\alpha$ and $C_\beta$ atoms as a C=C bond partially forms in the agostic structure.[21] The bond angle of Pd–C31–C32 for **2a** is 78.9(2)º, which is substantially smaller than the ideal angle of 109º for an $sp^3$ hybridized carbon. The acute angle at C31 ($C_\alpha$) suggests an attraction between Pd and C32 and is characteristic of the agostic interaction.

**Table 2. Comparison of Bond Parameters of β-Agostic (α-Diimine)Pd Complexes with Ni[7c] and Fe agostic complexes[22]**

| | **2a** (M = Pd) | **2b** (M = Pd) | M = Ni | M = Fe |
|---|---|---|---|---|
| M–C31 (Å) | 2.030(4) | | 1.901(4) | |
| M–C32 (Å) | 2.264(4) | | 2.081(5) | |
| C31–C32 (Å) | 1.469(6) | | 1.468(7) | |
| M–C31–C32 (º) | 78.9(2) | | 75.0(3) | |
| M–H34A (Å) | | 1.60(4) | 1.67(5) | 1.874(3) |
| C34–H34A (Å) | | 1.20(5) | 1.001(10) | 1.164(3) |

The bond lengths of Pd–H34A (agostic) and C34–H34A for **2b** are determined by neutron diffraction to be 1.60(4) Å and 1.20(5) Å, respectively (Table 2). Although insufficient precision prevented quantitative analysis, the short distance between Pd and H34A is comparable to that of the Ni analogue,[7c] and provides clear evidence for a bonding interaction between Pd and the agostic proton. It is noteworthy that the C34–H34A bond is stretched, whereas such elongation is not observed in the Ni analogue. Similar elongation has been reported in a Fe agostic complex, $[Fe(P(OCH_3)_3)_3(\eta^3\text{-}C_8H_{13})]^+[BF_4]^-$, and is attributed to a reduced C–H bond order.[22]

Variable temperature NMR measurements were conducted to elucidate the reason for the line-broadening observed in the $^1$H NMR spectrum of **2a**. The $^1$H resonances at –8.8 and 1.7 ppm, observed at –95 ºC, broadened as the temperature was increased and the peaks coalesced at –60 ºC (Figure S3). Above –60 ºC, a new peak appeared at –0.34 ppm and continued to sharpen as the temperature was increased. This signal corresponds to the averaged resonances of the ethyl group. The barrier ($\Delta G^‡$) for the exchange of the agostic $^a$H and the non-agostic α and β Hs was estimated to be 8.5 kcal/mol from the coalescence temperature using the fast exchange approximation.[23] Furthermore, **2a-$^{13}$C**, in which the carbons of the Pd-*Et* were labeled with $^{13}$C, exhibits two broad $^{13}$C NMR resonances at 37 and 19 ppm at –95 ºC (Figure S4). These peaks coalesced to a new peak at 29 ppm as the temperature was increased. An Eyring plot based on dynamic NMR analysis afforded kinetic parameters for the exchange of $C_\alpha$ and $C_\beta$ as $\Delta H^‡$ = 5.7 kcal/mol and $\Delta S^‡$ = –8.9 e.u. (e.u. = cal $mol^{-1}$ $T^{-1}$) (Figure 2).

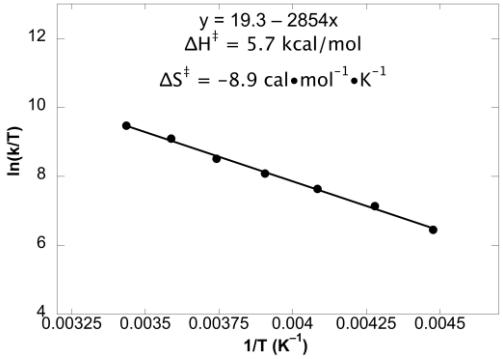


**Figure 2.** Eyring plots for β-H elimination of **2-$^{13}$C**.

The dynamic exchange evident in the NMR spectra can be attributed to the rotation of the β-methyl (Scheme 3A) and a sequential β-H elimination followed by hydride reinsertion (Scheme 3B). The kinetic barriers for β-methyl rotation and β-H elimination/reinsertion were 8.4 and 6.9 kcal/mol at –108 ºC, respectively, in Brookhart's initial Pd catalysts.[14e] Our kinetic results for **2a** match with these previous measurements. The barrier ($\Delta G^‡$) of 7.6 kcal/mol for β-H elimination and hydride reinsertion is significantly lower than that of the corresponding Ni complexes (14 kcal/mol).[7c] The lower barrier for β-H elimination, in combination with reversible olefin binding, accounts for the faster chain migration in Pd-catalyzed polymerization compared with Ni, result-

ing in a higher degree of branching in Pd-catalyzed polymerization.

**Scheme 3. Dynamic Processes of Pd Agostic Complexes and Their Kinetic Barriers**

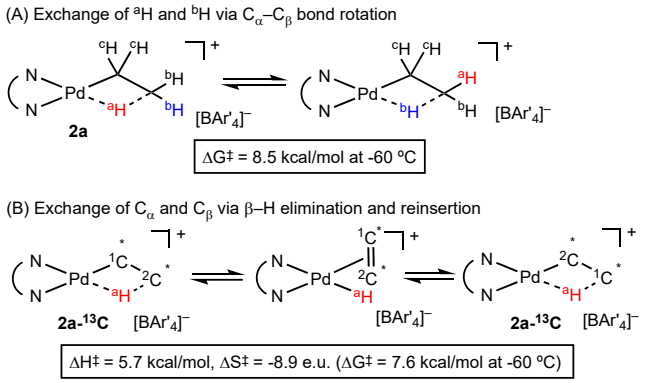


In summary, we have determined the structures of a series of β-agostic (α-diimine)Pd ethyl complexes by single crystal X-ray and neutron diffraction. The characteristically acute bond angle of Pd–$C_\alpha$–$C_\beta$ and short $C_\alpha$–$C_\beta$ bond distance provide clear evidence for a β-agostic interaction. Dynamic NMR analysis revealed that the barrier for β-H elimination and hydride reinsertion is 7.6 kcal/mol, significantly lower than that of the corresponding Ni analogue (14 kcal/mol). This observation is consistent with extensive and rapid chain migration in polymerizations catalyzed by Pd. Characterization of the agostic structure and the kinetic barrier for β-H elimination offer important insight into the mechanism of polymerization.

## ASSOCIATED CONTENT

**Supporting Information**. Experimental procedures, simulation, additional X-ray structures, and NMR spectra. This material is available free of charge via the Internet at http://pubs.acs.org.

## AUTHOR INFORMATION

### Corresponding Author

diao@nyu.edu

### Notes

The authors declare no competing financial interest.

## ACKNOWLEDGMENT

H.X. is grateful to the Weck group for assistance in characterizing polyethylene. This work was supported by the National Science Foundation (CHE-1654483). The X-ray diffraction facility is partially supported by the NSF (DMR-0820341 and DMR-1420073). The CPTCI-cryoprobe was acquired through the support of the NIH (OD016343). Neutron single crystal diffraction measurements were performed at the Spallation Neutron Source, a DOE Office of Science User Facility operated by the Oak Ridge National Laboratory, under Contract No. DE-AC05-00OR22725 with UT-Battelle, LLC.

## REFERENCES

1. For reviews, see: (a) Yao, W.; Eisenstein, O.; Crabtree, R. H. *Inorg. Chim. Acta* **1997**, *254*, 105-111. (b) Brookhart, M.; Green, M. L. H. *J. Organomet. Chem.* **1983**, *250*, 395-408. (c) Brookhart, M.; Green, M. L. H.; Wong, L.-L. In *Prog. Inorg. Chem.*; John Wiley & Sons, Inc.: 2007, p 1-124. (d) Brookhart, M.; Green, M. L. H.; Parkin, G. *Proc. Nat. Acad. Sci.* **2007**, *104*, 6908-6914.

2. Labinger, J. A.; Bercaw, J. E. *Nature* **2002**, *417*, 507-514.

3. (a) Parkin, G.; Bunel, E.; Burger, B. J.; Trimmer, M. S.; Van Asselt, A.; Bercaw, J. E. *J. Mol. Catal.* **1987**, *41*, 21-39. (b) Beletskaya, I. P.; Cheprakov, A. V. *Chem. Rev.* **2000**, *100*, 3009-3066.

4. For computational studies, see: (A) Romeo, R.; D'Amico, G.; Sicilia, E.; Russo, N.; Rizzato, S. *J. Am. Chem. Soc.* **2007**, *129*, 5744-5755. (b) Hasanayn, F.; Achord, P.; Braunstein, P.; Magnier, H. J.; Krogh-Jespersen, K.; Goldman, A. S. *Organometallics* **2012**, *31*, 4680-4692. (c) Pudasaini, B.; Janesko, B. G. *Organometallics* **2013**, *33*, 84-93. (d) Barquera-Lozada, J. E.; Obenhuber, A.; Hauf, C.; Scherer, W. *J. Phys. Chem. A* **2013**, *117*, 4304-4315. (e) Debnath, T.; Ash, T.; Banu, T.; Das, A. K. *Theor. Chem. Acc.* **2016**, *135*, 1-14.

5. For a representative example, see: Dawoodi, Z.; Green, M. L. H.; Mtetwa, V. S. B.; Prout, K.; Schultz, A. J.; Williams, J. M.; Koetzle, T. F. *J. Chem. Soc., Dalton Trans.* **1986**, 1629-1637.

6. For a representative example, see: Baratta, W.; Mealli, C.; Herdtweck, E.; Ienco, A.; Mason, S. A.; Rigo, P. *J. Am. Chem. Soc.* **2004**, *126*, 5549-5562.

7. (a) Conroy-Lewis, F. M.; Mole, L.; Redhouse, A. D.; Litster, S. A.; Spencer, J. L. *J. Chem. Soc., Chem. Commun.* **1991**, 1601-1603. (b) Kogut, E.; Zeller, A.; Warren, T. H.; Strassner, T. *J. Am. Chem. Soc.* **2004**, *126*, 11984-11994. (c) Xu, H.; White, P. B.; Hu, C.; Diao, T. *Angew. Chem. Int. Ed.* **2017**, *56*, 1535-1538.

8. (a) Carr, N.; Dunne, B. J.; Orpen, A. G.; Spencer, J. L. *J. Chem. Soc., Chem. Commun.* **1988**, 926-928. (b) Mole, L.; Spencer, J. L.; Carr, N.; Orpen, A. G. *Organometallics* **1991**, *10*, 49-52. (c) Spencer, J. L.; Mhinzi, G. S. *J. Chem. Soc., Dalton Trans.* **1995**, 3819-3824. (d) Crosby, S. H.; Clarkson, G. J.; Rourke, J. P. *J. Am. Chem. Soc.* **2009**, *131*, 14142-14143.

9. For γ-agostic Pd complexes, see: (a) Stambuli, J. P.; Incarvito, C. D.; Bühl, M.; Hartwig, J. F. *J. Am. Chem. Soc.* **2004**, *126*, 1184-1194. (b) Watanabe, C.; Iwamoto, T.; Kabuto, C.; Kira, M. *Angew. Chem. Int. Ed.* **2008**, *47*, 5386-5389. (c) Walter, M. D.; White, P. S.; Brookhart, M. *Chem. Commun.* **2009**, 6361-6363. (d) Thomas, H. R.; Deeth, R. J.; Clarkson, G. J.; Rourke, J. P. *Organometallics* **2011**, *30*, 5641-5648.

10. Johnson, L. K.; Killian, C. M.; Brookhart, M. *J. Am. Chem. Soc.* **1995**, *117*, 6414-6415.

11. (a) Ittel, S. D. In *Metalorganic Catalysts for Synthesis and Polymerization: Recent Results by Ziegler-Natta and Metallocene Investigations*; Kaminsky, W., Ed.; Springer Berlin Heidelberg: Berlin, Heidelberg, 1999, p 616-628. (b) Ittel, S. D.; Johnson, L. K.; Brookhart, M. *Chem. Rev.* **2000**, *100*, 1169-1204. (c) Domski, G. J.; Rose, J. M.; Coates, G. W.; Bolig, A. D.; Brookhart, M. *Prog. Polym. Sci.* **2007**, *32*, 30-92. (d) Guan, Z.; Popeney, C. S. In *Metal Catalysts in Olefin Polymerization* 2009, p 179-220. (e) Camacho, D. H.; Guan, Z. *Chem. Commun.* **2010**, *46*, 7879-7893.

12. L. K. Johnson, S. Mecking, M. Brookhart, *J. Am. Chem. Soc.* **1996**, *118*, 267-268.

13. Guan, Z.; Cotts, P. M.; McCord, E. F.; McLain, S. J. *Science* **1999**, *283*, 2059-2062.

14. (a) Mecking, S.; Johnson, L. K.; Wang, L.; Brookhart, M. *J. Am. Chem. Soc.* **1998**, *120*, 888-899. (b) Tempel, D. J.; Brookhart, M. *Organometallics* **1998**, *17*, 2290-2296. (c) Tempel, D. J.; Johnson, L. K.; Huff, R. L.; White, P. S.; Brookhart, M. *J. Am. Chem. Soc.* **2000**, *122*, 6686-6700. (d) Shultz, L. H.; Tempel, D. J.; Brookhart, M. *J. Am. Chem. Soc.* **2001**, *123*, 11539-11555. (e) Shultz, L. H.; Brookhart, M. *Organometallics* **2001**, *20*, 3975-3982.

15. For computational studies, see: (a) Michalak, A.; Ziegler, T. *Organometallics* **1999**, *18*, 3998-4004. (b) Michalak, A.; Ziegler, T. *J. Am. Chem. Soc.* **2001**, *123*, 12266-12278.

16. Brookhart, M.; Grant, B.; Volpe, A. F. *Organometallics* **1992**, *11*, 3920-3922.

17. Brookhart, M.; Hauptman, E.; Lincoln, D. M. *J. Am. Chem. Soc.* **1992**, *114*, 10394-10401.

18. Rummey, J. M.; Boyce, M. C. *J. Chem. Educ.* **2004**, *81*, 762-763.

19. (a) Popeney, C.; Guan, Z. *Organometallics* **2005**, *24*, 1145-1155. (b) Dai, S.; Sui, X.; Chen, C. *Angew. Chem. Int. Ed.* **2015**, *54*, 9948-9953.

20. Leatherman, M. D.; Svejda, S. A.; Johnson, L. K.; Brookhart, M. *J. Am. Chem. Soc.* **2003**, *125*, 3068-3081.

21. Silverstein, R. M.; Bassler, G. C.; Morrill, T. C. *Spectrometric Identification of Organic Compounds,* 5th ed.; Wiley: New York, 1991; p 247.

22. Brown, R. K.; Williams, J. M.; Schultz, A. J.; Stucky, G. D.; Ittel, S. D.; Harlow, R. L. *J. Am. Chem. Soc.* **1980**, *102*, 981-987.

23. Anet, F. A. L.; Bourn, A. J. R. *J. Am. Chem. Soc.* **1967**, *89*, 760-768.

TOC

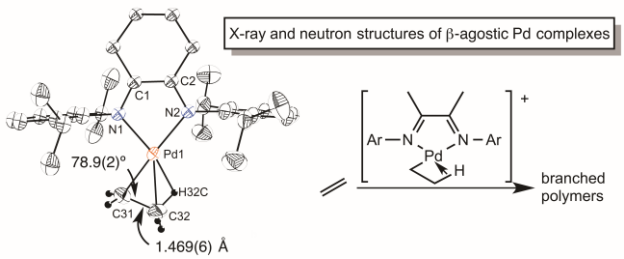
X-ray and neutron structures of β-agostic Pd complexes
C1
C2
N1
N2
Pd1
78.9(2)°
H32C
C31
C32
1.469(6) Å
Ar—N
N—Ar
Pd
H
+
branched
polymers